ACCOUNTS of chemical research

Article

pubs.acs.org/accounts

Mechanism of Rh-Catalyzed Oxidative Cyclizations: Closed versus Open Shell Pathways

Published as part of the Accounts of Chemical Research special issue "Computational Catalysis for Organic Synthesis".

Yoonsu Park, Seihwan Ahn, Dahye Kang, and Mu-Hyun Baik*

Center for Catalytic Hydrocarbon Functionalizations, Institute for Basic Science (IBS), Daejeon 305-701, Republic of Korea
Department of Chemistry, Korea Advanced Institute of Science and Technology (KAIST), Daejeon 305-701, Republic of Korea

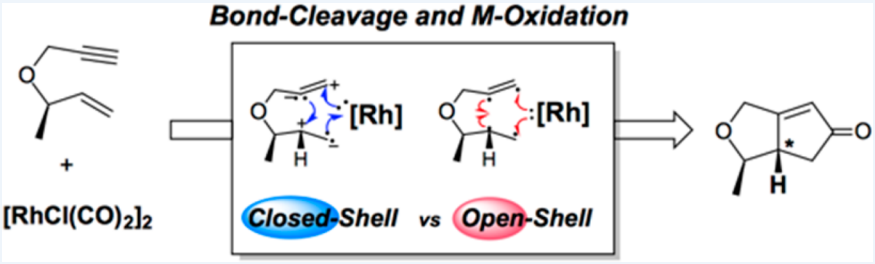

CONSPECTUS: A conceptual theory for analyzing and understanding oxidative addition reactions that form the cornerstone of many transition metal mediated catalytic cycles that activate C−C and C−H bonds, for example, was developed. The cleavage of the σ- or π-bond in the organic substrate can be envisioned to follow a closed or an open shell formalism, which is matched by a corresponding electronic structure at the metal center of the catalyst. Whereas the assignment of one or the other mechanistic scenario appears formal and equivalent at first sight, they should be recognized as different classes of reactions, because they lead to different reaction optimization and control strategies.

The closed-shell mechanism involves heterolytic bond cleavages, which give rise to highly localized charges to form at the transition state. In the open-shell pathway, bonds are broken homolytically avoiding localized charges to accumulate on molecular fragments at the transition states. As a result, functional groups with inductive effects may exert a substantial influence on the energies of the intermediate and transition states, whereas no such effect is expected if the mechanism proceeds through the open-shell mechanism. If these functional groups are placed in a way that opens an electronic communication pathway to the molecular sites where charges accumulate, for example, using hyperconjugation, electron donating groups may stabilize a positive charge at that site.

An instructive example is discussed, where this stereoelectronic effect allowed for rendering the oxidative addition diastereoselective. No such control is possible, however, when the open-shell reaction pathway is followed, because the inductive effects of functional groups have little to no effect on the stabilities of radical-like substrate states that are encountered when the bonds are broken in a homolytic fashion. Whether the closed-shell or open-shell mechanism for oxidative addition is followed is determined by the ordering of the d-orbital dominated frontier orbitals. If the highest occupied molecular orbital (HOMO) is oriented in space in such a way that will give the organic substrate easy access to the valence electron pair, the closed-shell mechanism can be followed. If the shape and orientation of the HOMO is not appropriate, however, an alternative pathway involving singlet excited states of the metal that will invoke the matching radicaloid cleavage of the organic substrate will dominate the oxidative addition. This novel paradigm for formally analyzing and understanding oxidative additions provides a new way of systematically understanding and planning catalytic reactions, as demonstrated by the in silico design of room-temperature Pauson−Khand reactions.

INTRODUCTION

Oxidative additions are ubiquitous among transition metal catalyzed organic transformations,[1] and they constitute one of the mechanistic cornerstones of many organometallic reaction mechanisms.[2] Conceptually, oxidative additions are reasonably well understood: As illustrated in Figure 1, they provide a convenient way of cleaving a covalent bond, such as a C−H bond,[3] by fragmenting the substrate and adding the molecular components to the reactive metal center as ligands.[4] C−H activation of an alkane may therefore give a metal hydrido-alkyl complex, as illustrated in Figure 1. Similarly, C−C bond cleavage and bond reorganization can afford useful C−C coupled products, as highlighted in Figure 1.[5] The oxidative coupling of an alkene with an alkyne gives a metalla-cyclopentene, for instance. During these processes, the metal

Received: March 1, 2016
Published: May 17, 2016

DOI: 10.1021/acs.accounts.6b00111
Acc. Chem. Res. 2016, 49, 1263−1270

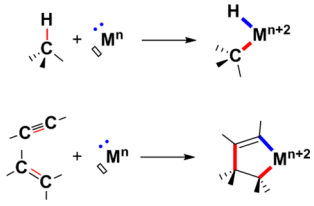

Figure 1. Two examples of substrate activation using oxidative addition.

center supplies two of the total of four or six electrons that are needed to form the oxidative addition products, as shown in blue in Figure 1. Consequently, the metal center is formally oxidized, and its oxidation state increases by +II. Despite being so important, there is currently no general concept that allows for rationally and systematically controlling the outcome of oxidative additions,[6] for example, by modifying the ligand composition or changing the identity of the metal center. It is impossible to rationally predict how modifications of the substrate will impact the reaction, requiring laborious, explicit tests to establish the substrate scope of the reaction. Similarly, it is practically impossible to rationally predict how the ligands or the metal center should be altered to increase the reactivity, given a moderately performing oxidative addition reaction. One obvious expectation is that when the metal center is made more electron-rich, the formal oxidation of the metal center may become easier to accomplish, which in turn may lead to more effective oxidative addition.[7] Whereas this reasoning leads to correct predictions in some instances,[8] it cannot be generalized. It is highly desirable to have a conceptual theory at hand that allows for qualitatively understanding and planning oxidative additions in general. The power of such a conceptual theory has long been demonstrated, for example, by the Woodward–Hoffmann rules[9] that allowed for qualitatively understanding pericyclic reactions.

Quantum chemical reaction modeling has become an important tool of mechanistic investigations over the last few decades.[10] In particular, density functional methods[11] are now considered standard for simulating organometallic reactions, which pose significant challenges to computer models due to the intrinsic complexity in electronic structure that transition metals introduce. Whereas currently available technology is far from being quantitatively reliable, significant insight can be gained by carefully carrying out computational studies and, perhaps more importantly, analyzing the results in detail and drawing practically useful conclusions. DFT has been used extensively to analyze oxidative addition reactions, but a unifying conceptual theory has not emerged.[12] This Account aims to highlight an approach toward developing such a unifying concept based on molecular orbital analysis.

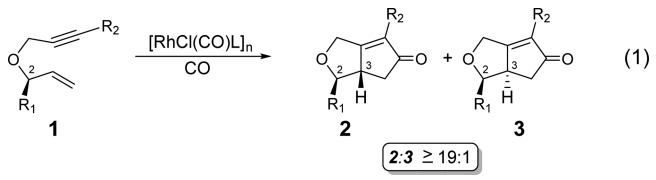

(1)

DISCUSSION

One instructive series of studies that highlight key challenges and a possible approach for developing a general concept for oxidative addition reactions was reported for a Rh-catalyzed Pauson–Khand reaction [eq 1]. Formally a [2 + 2 + 1] carbocyclization involving a 1,6-enyne substrate **1** and carbon monoxide, this transformation afforded the corresponding bicycle **2** with exquisite diastereocontrol.[13] The stereochemical outcome was rationalized as illustrated in Figure 2. The key step in the mechanism involves the oxidative addition of the enyne substrate to the metal to give a metallacyclopentene intermediate. The orientation of the R_1 group on the chiral C2-position was envisioned to give preference to the metal fragment binding to the "backside" of the enyne functionality as illustrated in intermediate **i** in Figure 2. The alternative binding as shown in the diastereomer **ii** was thought to be higher in energy due to steric interactions between the ML_n and R_1 functionalities. The η^2-binding of the metal to the enyne moiety may determine the stereochemical outcome, as intermediate **i** may cyclize to give **iii**, while oxidative coupling will produce **iv** from **ii**. This explanation follows the tradition of invoking nonbonded interactions between the key components of the reactive species to energetically discriminate between two possible reaction pathways based on sterically demanding molecular configurations. This proposed rationale is highly representative of how stereoselective reactions are analyzed and understood in organic reaction design; in lieu of more precise experimental or computational data, this explanation is reasonable. There is a serious fundamental problem with this line of reasoning, however: justifying the diastereoselectivity solely based on the energetics of the reactant adducts and the resulting relative population of adduct species in the

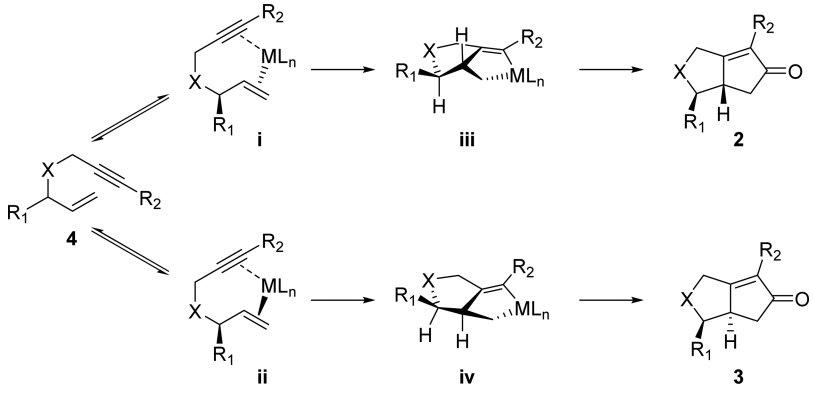

Figure 2. Rationalization of the stereochemical outcome of the Pauson–Khand reaction. Adapted from ref 13. Copyright 2001 American Chemical Society.

DOI: 10.1021/acs.accounts.6b00111
Acc. Chem. Res. 2016, 49, 1263–1270

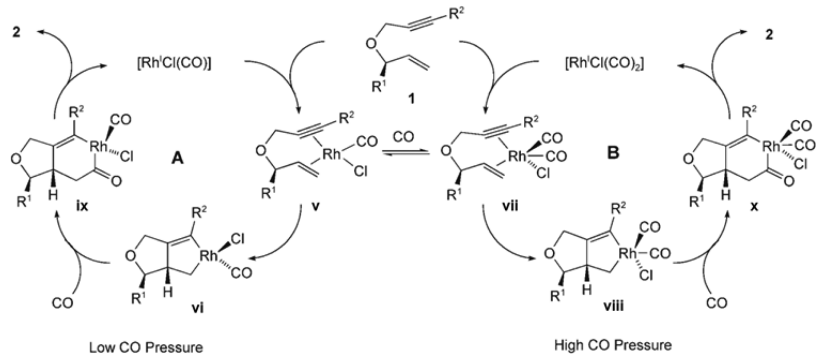

Figure 3. Mechanism of Rh-catalyzed Pauson–Khand annulation. Adapted from ref 14. Copyright 2008 Wiley VCH.

equilibrium is strictly only valid if the reaction is under thermodynamic control. That is, the barrier of cyclization must be identical or nearly so for both diastereomers and reversible, such that the initial energy difference of the adducts are preserved throughout the reaction pathway at the transition and product states. If the transition state of the minor reactant adduct species is lower in energy than that of the major adduct, the relative population difference in favor of the major reactant at the beginning of the reaction becomes meaningless, because the minor component of the equilibrium will be removed from the equilibrium more quickly due to said faster rate of product formation. Removal of the minor component of the reactant equilibrium will quickly lead to an adjustment of the reactant populations in equilibrium, where the minor reactant molecule will be reformed according to the equilibrium constant. Over time, all of the major reactant will be transformed to the minor reactant, which is siphoned away from the equilibrium to give the unexpected product.

Second, the oxidative addition resulting in the metallacycle is likely irreversible, which diminishes the impact of the thermodynamic preference of one diastereomer over the other, since kinetic factors will become much more important for determining the product distribution due to such a nonequilibrium condition. Lastly, the sterically induced discrimination of **ii** over **i** is expected to vanish at the transition state in the aforementioned reaction, because the metal fragment will migrate into the molecular plane defined by the enyne moiety as the molecule traverses the transition state and the sterically challenging interaction between the metal fragment and the R_1 group will be minimized.

For these reasons, the diastereoselective Pauson–Khand reaction was examined in more detail using a quantum chemical molecular model, which suggested a very different explanation for controlling the diastereoselectivity.[14] Surprisingly, it was found that the number of carbonyl ligands on rhodium plays a critical role. Figure 3 illustrates the mechanism of carbocyclization using both a four- and five-coordinate rhodium center, determined by the number of carbonyl ligands on the metal center. Because the experiments are carried out with excess amounts of CO in solution, both catalyst isomers are expected to coexist in solution. The sequence of reaction steps in the catalytic cycle is identical; namely, the reactant complex **v** and **vii** first engage in oxidative addition to form the metallacycles **vi** and **viii**, respectively, followed by migratory insertion of CO into the Rh–C bond and reductive elimination to close the catalytic cycle. Cycle **A** is expected to be operative when the CO pressure is low, whereas high CO pressure should enable cycle **B**. Interestingly, the diastereoselectivity profiles were found to be vastly different. If the four-coordinate Rh-center is assumed to be the catalytically active species (cycle **A**), the DFT calculations indicate no diastereoselectivity, as shown in Figure 4. The transition states of the oxidative addition step, **v-TS** and **v-TS′**, were found to be at ∼28 kcal/mol for both diastereomers. This result is not in agreement with the experimental observation, because the nearly identical barriers suggest that both diastereomers should be formed. If the five-coordinate Rh-center is taken as the catalytically competent species, however, the DFT calculations suggested that the transition state leading to the experimentally observed product, **vii-TS**, is located at 26.6 kcal/mol, whereas the experimentally not observed product is associated with a much higher barrier of 33.6 kcal/mol associated with the transition state **vii-TS′**, as illustrated in Figure 5.

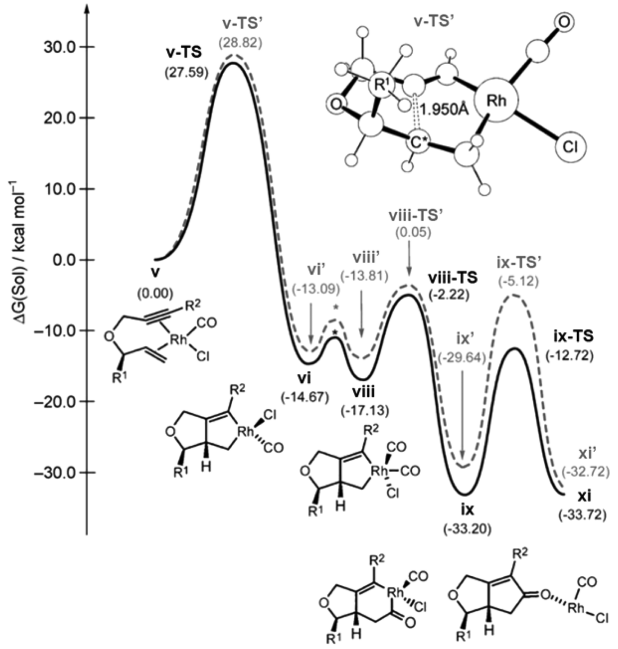

Figure 4. Reaction energy profile of the reaction using a four-coordinate Rh-catalyst, cycle **A** in Figure 3. Adapted from ref 14. Copyright 2008 Wiley VCH.

Because the four- and five-coordinate rhodium complexes coexist in solution with the five-coordinate complex being higher in energy, these results suggest that the diastereoselectivity should be dependent on the CO pressure. The five-coordinate rhodium catalyst is accessed more readily at high concentrations of CO, forcing the majority of the reaction to

DOI: 10.1021/acs.accounts.6b00111
Acc. Chem. Res. 2016, 49, 1263–1270

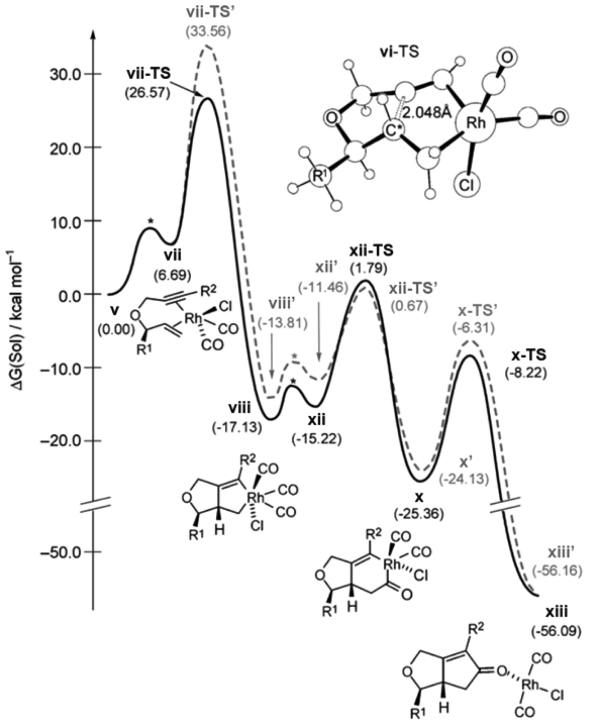

Figure 5. Reaction energy profile of the reaction using a five-coordinate Rh-catalyst, cycle **B** in Figure 3. Adapted from ref 14. Copyright 2008 Wiley VCH.

follow the pathway highlighted in Figure 5, giving high levels of diastereocontrol. At low concentrations of CO, the reaction pathway shown in Figure 4 becomes more relevant and, consequently, loss of diastereoselectivity should be observed. This provocative proposal from the computer model was challenged experimentally:[14] Instead of carrying out the carbocyclization under CO atmosphere, the reaction was performed with varying compositions of argon and carbon monoxide, as summarized in Table 1. In excellent agreement

Table 1. Diastereomeric Ratios with Varying CO/Ar Gas Composition[a]

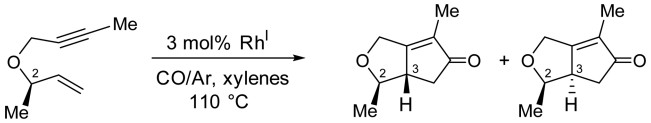

1a 2a 3a

		pressure [atm]			
entry	rhodium complex[b]	CO	Ar	yield[c] [%]	dr[d] **2a**/**3a**
1	[{RhCl(CO)$_2$}$_2$]	1.00	0.00	81	22:1
2	[{RhCl(CO)$_2$}$_2$]	0.10	0.90	64	10:1
3	[{RhCl(CO)$_2$}$_2$]	0.05	0.95	57	6:1
4	[{RhCl(CO)(dppp)}$_2$]	1.00	0.00	88	≥99:1
5	[{RhCl(CO)(dppp)}$_2$]	0.10	0.90	51	58:1
6	[{RhCl(CO)(dppp)}$_2$]	0.05	0.95	44	57:1

Adapted from ref 14. Copyright 2008 Wiley VCH. [a]All reactions were carried out on a 0.25 mmol reaction scale utilizing 3 mol % of the rhodium complex in xylene at 110 °C. [b]dppp = 1,3-bis-(diphenylphosphanyl)propane. [c]Isolated yields. [d]Ratios of diastereoisomers were determined by capillary GLC analysis on the crude reaction mixtures.

with the predictions from the computer model, the diastereomeric ratio decreased to 10:1 and 6:1 when the CO gas content was reduced to 10% and 5%, respectively. Thus, a plausible picture that emerges from the computational and experimental results is that Rh is forced by Le Chatelier's principle to carry an additional CO ligand at high concentrations of CO, thus, accessing the diastereoselective reaction pathways involving the five-coordinate Rh-catalyst, illustrated in Figure 5. When the CO concentration is low, the four-coordinate Rh-complex is the dominating reactant complex and the carbocyclization reaction loses diastereoselectivity, as the reaction follows the pathway summarized in Figure 4.

The difference in stereoselectivity as the composition of the Rh-catalyst is varied offers a unique opportunity for systematically examining the electronic structure that gives rise to the dramatically different stereochemical behavior in the reaction.[15] Although the chemical steps in the catalytic cycle seem identical on first sight, the oxidative addition promoted by the five-coordinate Rh-complex is fundamentally different from the same reaction mediated by the four-coordinate Rh-analogue. Figure 6 provides an intuitive summary of the diastereoselective

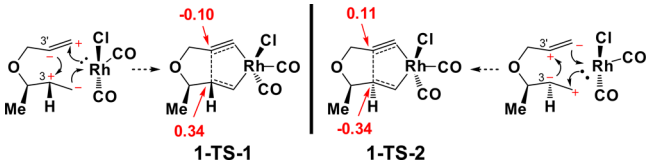

Figure 6. Partial charges of the two transition states found using the five-coordinate Rh-complex. Adapted from ref 15. Copyright 2011 American Chemical Society.

metallacarbocycle forming event using the five-coordinate Rh-complex. The transition state **1-TS-1** leads to the experimentally observed diastereomer, whereas **1-TS-2** gives the diastereomer that is not observed. Interestingly, the computed partial charges at the C3 and C3′ positions of the enyne in the transition state **1-TS-1** are +0.34 and −0.10, but in **1-TS-2** they are −0.34 and +0.11, respectively. These charge polarizations can be rationalized easily by invoking a heterolytic cleavage of the double and triple bonds in such a way that places the appropriate charges on the C3 and C3′ positions. To complete the carbocyclization, the electron pairs can be formally pushed as shown in Figure 6 to form a new C−C bond between the C3 and C3′, and two Rh−C bonds that constitute the metallacyclopentene skelton. Note that four of the six electrons needed to form the metallacyclopentene are supplied by the double and triple bonds of the enyne, but the other two electrons are recruited from the metal valence shell. This promotion of two electrons from the purely metal-based valence shell into the metal−ligand bonding framework constitutes the oxidative component of the oxidative addition.

The "arrow pushing" scheme, shown in Figure 6, is a common tool used frequently to rationalize bond reorganizations in organic reactions. Typically, they are not given a physical meaning and are thought of as strictly formal. Whereas we do not mean to suggest that these conceptual drawings depict faithfully the flow of electrons, they appear to provide a useful cartoon of the polarization characteristics found at the transition state. Figure 7 illustrates the stereoelectronic reason for the different charge polarization that we propose to be responsible for the diastereoselectivity. The only way to obtain

DOI: 10.1021/acs.accounts.6b00111
Acc. Chem. Res. 2016, 49, 1263−1270

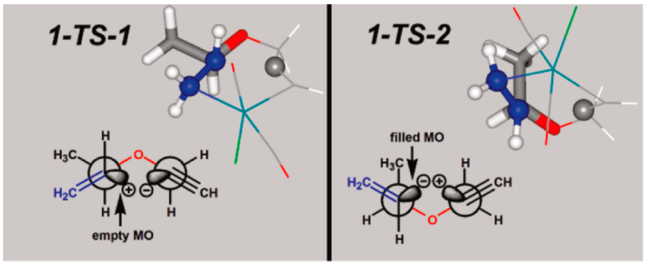

Figure 7. Computed structures of the transition states **1a-TS-1** and **1a-TS-2** and their Newman projections. Adapted from ref 15. Copyright 2011 American Chemical Society.

the diastereomer, in which the R-group on C2 and the hydrogen on C3 are in a *syn* orientation to each other, is to go through a structural arrangement at the transition state that places the C3−C3′ vector in an *anti*-disposition to the R-group on C2, as illustrated in Figure 7 for **1-TS-1**. As a result, the inductive effect of the R-group can be imposed on the C3-carbon via hyperconjugation. This electronic communication of the inductive effect stabilizes a cationic charge on the C3-carbon. Figure 7 also shows the analogous stereoelectronic effect in the transition state **1-TS-2**, which would give the metallacyclopentene diastereomer with the C2−R and C3−H groups in *anti* orientation to each other. To obtain the *anti*-configuration, the C3−C3′ vector must be placed in a nearly perfect orthogonal disposition to the C2−R bond. Because there is no hyperconjugation pathway of electronic communication between the C2−R group and the C3-based *sp*-hybrid orbital that will promote the C3−C3′ bond formation, no stabilizing impact from the inductive effect of the C2−R group can be felt in this transition state. As a result, the double bond of the alkene is cleaved to produce a cationic carbon center at the terminal position, placing the negative charge on the C3-position, as illustrated in Figure 7. These stereoelectronic effects ultimately stabilize the transition state **1-TS-1** over **1-TS-2**.

Figure 8 compares the partial charges found at the two transition states using the four-coordinate Rh-complexes, **1-TS-3** and **1-TS-4**, leading to the *syn* and *anti* products, respectively. Interestingly, the C3-carbons have partial charges of 0.04 and 0.05, respectively, and the C3′ carbons show partial charges of −0.04 and 0.10, respectively. Compared with the charges seen with the five-coordinate Rh-complexes, these partial charges are much reduced. One plausible way of rationalizing this dramatic difference is invoking an open-shell mechanism of bond cleavage, as highlighted in Figure 8 using the familiar "arrow pushing" formalism. This homolytic bond cleavage process will not give rise to any partial charge accumulation.

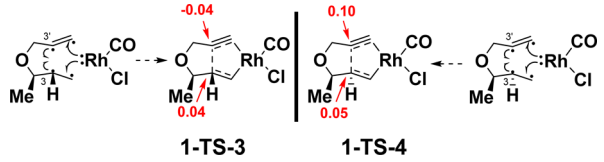

Figure 8. Partial charges of the two transition states found using the four-coordinate Rh-complex.

Whereas the overall mechanism is identical, the closed and open-shell reaction pathways present notably different characteristics and demand vastly different reaction optimization strategies. Since the dipole moment of the molecule will increase significantly when the transition state is traversed, the closed-shell reaction will be sensitive to the polarity of the solvent. The reaction rate is expected to increase in polar solvents, whereas the open-shell reaction will prefer nonpolar solvents. More importantly, functional groups with inductive effects placed at strategic positions will change the shape of the reaction energy profile significantly giving rise to the exquisite diasterocontrol in this case. Oxidative additions based on open-shell mechanisms, however, are not expected to be sensitive to the electronic effects of the functional groups, as demonstrated by the computed reaction energy profile shown in Figure 4. The aforementioned experimental confirmation of the prediction based on this model, namely, that lowering the CO pressure will reduce the diastereoselectivity, is a convincing support for this mechanistic interpretation.

But why does the five-coordinate Rh-complex undergo oxidative addition via a closed-shell pathway, when the four-coordinate Rh-complex follows an open-shell route? Figure 9

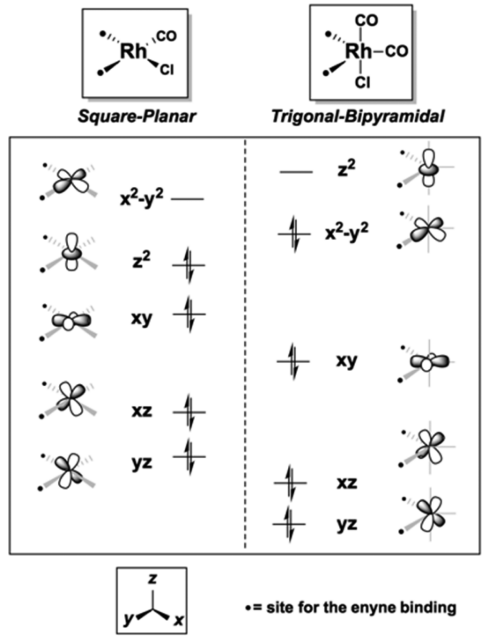

Figure 9. MO diagram of a square-planar vs trigonal bipyramidal Rh(I)-complex.

shows a conceptual MO diagram for the square-planar four-coordinate and the trigonal-bipyramidal five-coordinate Rh(I)-complexes. In the former case, the HOMO is the d_{z^2} orbital and the LUMO is the $d_{x^2-y^2}$ orbital. Conversely, the HOMO in the trigonal-bipyramidal five-coordinate Rh(I) complex is the $d_{x^2-y^2}$ orbital, and the LUMO becomes the d_{z^2} orbital, as illustrated in Figure 9. In both complexes, the enyne substrate binds in the equatorial position, as indicated in Figure 9. Because the trigonal-bipyramidal Rh(I) complex presents a filled $d_{x^2-y^2}$ orbital to the enyne ligand, the oxidative addition can proceed and the valence electrons of the metal in the $d_{x^2-y^2}$ orbital can participate in the metallacylopentene formation. In the square-planar four-coordinate Rh-complex, the $d_{x^2-y^2}$ orbital is empty and cannot promote oxidative addition in a similar fashion. Instead, this Rh-complex must utilize its lowest singlet excited state, where one of the HOMO electrons is promoted to the LUMO to afford an open-shell singlet state. Naturally, this catalyst will enforce an open-shell oxidative addition pathway.

DOI: 10.1021/acs.accounts.6b00111
Acc. Chem. Res. 2016, 49, 1263−1270

This proposed new paradigm for understanding the relationship between metal coordination geometry, its electronic structure, and the mechanism of metallacarbocyclization is reminiscent of the orbital symmetry arguments used in the Woodward−Hoffmann rules.[9] Just as the thermally driven pericyclic reaction requires the HOMO and LUMO symmetries of the substrates to match, so must the HOMO symmetry of the transition metal valence shell match the symmetry of the organic substrate, as it undergoes heterolytic bond cleavage, exposing positively and negatively charged molecular fragments. The negatively charged fragment acts as a Lewis base, demanding the metal center to act as a Lewis acid when forming the M−L bond. The positively charged substrate site becomes responsible for the oxidative component of the oxidative addition by recruiting a valence electron pair from the metal center to form its M−L bond. If the coordination geometry of the metal center is such that the frontier orbital that has the proper symmetry is empty and cannot engage in a closed-shell mechanism, the oxidative addition can proceed using an open-shell mechanism, where electrons from lower lying d-orbitals are elevated. These formally excited states of the metal center will engage the substrate by enforcing a homolytic bond cleavage. This pathway is equivalent to the light-driven pericyclic reactions. One critically important consequence of this difference in electronic structure is that the closed-shell pathway allows for functional groups with inductive effects placed at certain positions to exert a stereoelectronic effect on the energetics of the intermediates and transition states. The open-shell pathway, however, does not offer such opportunity for reaction control.

The recognition that the diastereoselective version of the Pauson−Khand reaction described above involves a highly polarized transition state leads to an interesting exploitation strategy: If the placement of a functional group with inductive effects can discriminate one of the diastereomeric pathways by as much as 7 kcal/mol, as illustrated in Figure 5, and the control mechanism discussed above constitutes a more general paradigm, it should be possible to add other functional groups in such a way that lowers the reaction barrier without losing the diastereoselectivity. If the effect is strong enough, this may be one way to allow the oxidative addition to complete at room temperature. The requirement of elevated reaction temperature of at least 150 °C is a major problem, because it prevents this methodology from being utilized in the later stages of complex natural product synthesis to install stereocenters. Because the computer model was the basis of the generalized theory, it should also be possible to use the same computational models for a virtual screening study of different functional groups. This strategy is particularly attractive, because the computational screening is relatively easy when the full catalytic cycle has already been constructed. Several functionalized substrates were identified as interesting targets. Most interestingly, adding electron withdrawing halogen groups to the terminal position of the alkyne moiety and thereby increasing the positive partial charge at the C3′ position emerged as a promising target. The reaction barriers for forming the *syn* product were calculated to be 24.5, 24.5, and 25.7 kcal/mol for the Cl, Br, and I substituted with enyne substrates,[14] which are notably lower than the barrier of 28.4 kcal/mol computed for the unsubstituted 1,6-enyne (Table 2). The diastereoselectivity was predicted to be maintained throughout, as indicated by the markedly higher barriers for the putative reaction leading to the *anti* diastereomer. In addition to the low reaction barriers that may afford room temperature carbocyclizations, the installment of halogen groups on the bicyclic products is attractive, because they provide convenient synthetic handles for further functionalizations. Subsequent experimental studies using the Cl-substituted alkyne confirmed these predictions with several slightly modified substrates (Table 3). For example, the ether-tethered 1,6-enyne carrying a methyl group at the chiral C2-position and the chloride group at the C4′-position gave a yield of 82% and a diastereomeric ratio of 98:2 in favor of the *syn* product.

Table 2. Effect of the C4′ Substituent on the Computed Barrier of Metallacycle Formation

		$\Delta G^{\ddagger}_{calc}$ (kcal/mol)	
entry	R_2	*syn* **2**	anti **3**
1	H	28.4	31.1
2	Cl	24.5	29.3
3	Br	24.5	29.5
4	I	25.7	30.3

Adapted from ref 15. Copyright American Chemical Society 2011.

Table 3. Scope of the Rhodium-Catalyzed Pauson−Khand Reaction with C4′-Halogenated 1,6-Enynes[a]

	1,6-enyne **1**				
entry	X	R_1	R_2	yield (%)[b]	ratio of **2**/**3**[c]
1	O	H	H	NR[d]	
2	O	H	Cl	74	
3	O	H	Br	39	
4	O	H	I	NR[d]	
5	$C(CO_2Me)_2$	H	Cl	74	
6	NTs	H	Cl	81	
7	NTs	Me	Cl	80	97:3
8	NTs	CH_2OBn	Cl	73	98:2
9	NTs	Bn	Cl	84	≥99:1
10	O	Me	Cl	82	98:2
11	O	CH_2OBn	Cl	84	≥99:1
12	O	Bn	Cl	87	≥99:1

Adapted from ref 15. Copyright American Chemical Society 2011. [a]All reactions were carried out on a 0.2 mmol scale utilizing 5 mol % $[RhCl(CO)_2]_2$ in *p*-xylene (0.1 M) at 25 °C. [b]Isolated yields. [c]Ratios of diastereoisomers were determined by HPLC or GC analysis of the crude products. [d]No reaction.

Whereas the agreement between theory and experiment regarding the qualitative prediction that the C4′-halogenation should lead to room temperature Pauson−Khand reaction is remarkable, the diastereometric ratio of ∼100:1 is not consistent with the computed energy difference of ∼5 kcal/mol between the two transition states (Table 2), as a much greater preference of the *syn* product, in the order of ∼10,000:1 should be found based on this energy difference. One possible explanation is that the intrinsic uncertainties of the computational model, including inaccuracies of the exchange−correlation functional, the approximate way entropy terms are treated, and errors in the evaluation of the solvation energy, make it unreasonable to expect a better agreement between theory and experiment. Whereas it is currently not possible to accurately assess how large these intrinsic errors are in reality and this issue remains a much debated topic in the computational chemistry community, there is also a simple chemical problem to consider: As discussed above, the binding

DOI: 10.1021/acs.accounts.6b00111
Acc. Chem. Res. 2016, 49, 1263−1270

of the additional carbon monoxide molecule to access the five-coordinate Rh-complex is an endergonic process, estimated to be ∼7 kcal/mol uphill. Thus, even with relatively high concentrations of CO in solution, the majority of the Rh-complexes will remain in the 4-coordinate configuration. The reaction barrier to form the *anti* diastereomer product from this intermediate is calculated to be 28.8 kcal/mol, which is markedly lower in energy than 31.1 kcal/mol calculated for the five-coordinate Rh-complex. Thus, the most consistent interpretation of the computed results is that the *syn* product is formed mainly by the five-coordinate Rh-complex, as shown in Figure 5. The *anti* product, however, is most likely formed by the four-coordinate Rh-complex. The computed energy difference between the two transition states of this reaction is therefore 2.2 kcal/mol, which is in excellent agreement with the experimentally determined diastereomeric ratio of ∼100:1.

■ CONCLUSIONS

The electronic foundation for oxidative addition reaction was examined and conceptualized based on the required disruptions of bonding framework in the organic substrate that may lead to localized charges when the bonds are broken heterolytically. The homolytic alternative to the bond breaking gives no localized charges but gives radicaloid intermediate states. The valence shell molecular orbitals of the Rh(I)-center are capable of promoting oxidative additions in both pathways. This formal and conceptual decomposition of the oxidative addition process is useful, because it should in principle enable a rational design of these important reactions. Two examples of such predictive use of the concept combined with high level DFT calculations demonstrate the potential for this novel way of analyzing and understanding oxidative additions: In the first case, the stereoelectronic basis for the diastereoselectivity was revealed, which allowed for predicting that the lowering of the CO pressure will afford loss of diastereocontrol. In the second example, a nontrivial halogenation of the alkyne moiety was predicted to lead to a room temperature reaction.

■ AUTHOR INFORMATION

Corresponding Author

*E-mail: mbaik2805@kaist.ac.kr.

Funding

We thank the Research Corporation (Scialog Award to M.H.B.) and the Institute for Basic Science (IBS-R10-D1) in Korea for financial support.

Notes

The authors declare no competing financial interest.

Biographies

Yoonsu Park obtained his B.S. degree in Chemistry at KAIST in 2014. He is currently a Ph.D. candidate under the joint supervision of Prof. Sukbok Chang and Prof. M.-H. Baik at the same university. His research interests are focused on the development and the fundamental understanding of organometallic catalysis.

Seihwan Ahn was born in Ulsan (Republic of Korea) in 1987. He received his B.S. degree in chemistry from Kyungpook National University (in Daegu, Korea) in 2012. He is currently a Ph.D. student under the supervision of Prof. M.-H. Baik at the Korea Advanced Institute of Science and Technology (KAIST) working on development of new organometallic reactions using computational approaches.

Dahye Kang was awarded her B.S. degree in Chemistry at KAIST in 2013. She is currently a Ph.D. student under the joint supervision of Prof. Sungwoo Hong and Prof. M.-H. Baik at KAIST. Her research interests include the development of new organometallic reactions and the mechanistic understanding of organometallic catalysis using computational molecular modeling techniques.

Mu-Hyun Baik received his Vordiplom (=Bachelor degree) from the Heinrich-Heine-Universität Düsseldorf (Germany) in 1994 and his Ph.D. from the University of North Carolina in Chapel Hill in 2000. After completing his postdoctoral training at Columbia University in New York, he was appointed an assistant professor of chemistry at Indiana University Bloomington in 2003. In 2008, he was promoted to associate professor of chemistry with tenure at Indiana University. In 2015, he moved to Korea to become an associate director of the Center for Catalytic Hydrocarbon Functionalizations within the Institute for Basic Science (IBS) and was appointed a professor of chemistry at the Korea Advanced Institute of Science and Technology (KAIST) in Daejeon, Korea.

■ REFERENCES

(1) Rendina, L. M.; Puddephatt, R. J. Oxidative Addition Reactions of Organoplatinum(II) Complexes with Nitrogen-Donor Ligands. *Chem. Rev.* **1997**, *97*, 1735−1754.

(2) (a) Hartwig, J. F. *Organotransition Metal Chemistry: From Bonding to Catalysis*; University Science Books: Sausalito, CA, 2010. (b) Niu, S.; Hall, M. B. Theoretical Studies on Reactions of Transition-Metal Complexes. *Chem. Rev.* **2000**, *100*, 353−406. (c) Ozerov, O. V. Oxidative Addition of Water to Transition Metal Complexes. *Chem. Soc. Rev.* **2009**, *38*, 83−88. (d) Goossen, L. J.; Koley, D.; Hermann, H. L.; Theil, W. Mechanistic Pathways for Oxidative Addition of Aryl Halides to Palladium(0) Complexes: A DFT Study. *Organometallics* **2005**, *24*, 2398−2410. (e) Matsubara, T.; Hirao, K. Density Functional Study on the Mechanism of the C−X (X = Sn, Ge, Si, C, H) σ Bond Oxidative Addition of HC≡CR (R = SnH_3, GeH_3, SiH_3, CH_3, H) to the $(PH_3)_2M$ (M = Ni, Pd, Pt) Complexes. Does the Substrate Approach the Metal in a Parallel or Perpendicular Manner? *Organometallics* **2002**, *21*, 4482−4489.

(3) (a) Arndtsen, B. A.; Bergman, R. G.; Mobley, T. A.; Peterson, T. H. Selective Intermolecular Carbon-Hydrogen Bond Activation by Synthetic Metal Complexes in Homogeneous Solution. *Acc. Chem. Res.* **1995**, *28*, 154−162. (b) Balcells, D.; Clot, E.; Eisenstein, O. C−H Bond Activation in Transition Metal Species from a Computational Perspective. *Chem. Rev.* **2010**, *110*, 749−823. (c) Ackermann, L. Carboxylate-Assisted Transition-Metal-Catalyzed C−H Bond Functionalization: Mechanism and Scope. *Chem. Rev.* **2011**, *111*, 1315−1345.

(4) Labinger, J. A.; Bercaw, J. E. Understanding and Exploiting C−H Bond Activation. *Nature* **2002**, *417*, 507−514.

(5) Souillart, L.; Cramer, N. Catalytic C−C Bond Activations via Oxidative Addition to Transition Metals. *Chem. Rev.* **2015**, *115*, 9410−9464.

(6) Portnoy, M.; Milstein, D. Chelate Effect on the Structure and Reactivity of Electron-Rich Palladium Complexes and Its Relevance to Catalysis. *Organometallics* **1993**, *12*, 1655−1664.

(7) (a) Xue, L.; Lin, Z. Theoretical Aspects of Palladium-Catalysed Carbon−Carbon Cross-Coupling Reactions. *Chem. Soc. Rev.* **2010**, *39*, 1692−1705. (b) van Leeuwen, P. W. N. M.; Kamer, P. C. J.; Reek, J. N. H.; Dierkes, P. Ligand Bite Angle Effects in Metal-Catalyzed C−C Bond Formation. *Chem. Rev.* **2000**, *100*, 2741−2770. (bb) Ess, D. H.; Gunnoe, T. B.; Cundari, T. R.; Goddard, W. A., III; Periana, R. A. Ligand Lone-Pair Influence on Hydrocarbon C−H Activation: A Computational Perspective. *Organometallics* **2010**, *29*, 6801−6815. (c) Wang, D. Y.; Choliy, Y.; Haibach, M. C.; Hartwig, J. F.; Krogh-Jespersen, K.; Goldman, A. S. Assessment of the Electronic Factors Determining the Thermodynamics of "Oxidative Addition" of C−H and N−H Bonds to Ir(I) Complexes. *J. Am. Chem. Soc.* **2016**, *138*,

DOI: 10.1021/acs.accounts.6b00111
Acc. Chem. Res. 2016, 49, 1263−1270

149−163. (d) Conradie, J.; Swarts, J. C. Oxidative Addition of CH_3I and CO Migratory Insertion in a Series of Ferrocene-Containing Carbonyl Phosphine β-Diketonato Rhodium(I) Complexes. *Organometallics* **2009**, *28*, 1018−1026. (e) Lam, K. C.; Marder, T. B.; Lin, Z. DFT Studies on the Effect of the Nature of the Aryl Halide Y−C_6H_4−X on the Mechanism of Its Oxidative Addition to Pd^0L versus Pd^0L_2. *Organometallics* **2007**, *26*, 758−760. (f) Barder, T. E.; Walker, S. D.; Martinelli, J. R.; Buchwald, S. L. Catalysts for Suzuki−Miyaura Coupling Processes: Scope and Studies of the Effect of Ligand Structure. *J. Am. Chem. Soc.* **2005**, *127*, 4685−4696.

(8) (a) Sargent, A. L.; Hall, M. B.; Guest, M. F. Theoretical Studies of Inorganic and Organometallic Reaction Mechanisms. 3. The Origin of the Difference in the Barrier for the Kinetic and Thermodynamic Products for the Oxidative Addition of Dihydrogen to a Square-Planar Iridium Complex. *J. Am. Chem. Soc.* **1992**, *114*, 517−522. (b) Cheong, M.; Ziegler, T. Density Functional Study of the Oxidative Addition Step in the Carbonylation of Methanol Catalyzed by $[M(CO)_2I_2]^-$ (M = Rh, Ir). *Organometallics* **2005**, *24*, 3053−3058. (c) Griffin, T. R.; Cook, D. B.; Haynes, A.; Pearson, J. M.; Monti, D.; Morris, G. E. Theoretical and Experimental Evidence for S_N2 Transition States in Oxidative Addition of Methyl Iodide to *cis*-$[M(CO)_2I_2]^-$ (M = Rh, Ir). *J. Am. Chem. Soc.* **1996**, *118*, 3029−3030. (d) Conradie, M. M.; Conradie, J. Methyl Iodide Oxidative Addition to [Rh(acac)(CO)-(PPh_3)]: an Experimental and Theoretical Study of the Stereochemistry of the Products and the Reaction Mechanism. *Dalton Trans.* **2011**, *40*, 8226−8237. (e) Ess, D. H.; Nielsen, R. J.; Goddard, W. A., III; Periana, R. A. Transition-State Charge Transfer Reveals Electrophilic, Ambiphilic, and Nucleophilic Carbon−Hydrogen Bond Activation. *J. Am. Chem. Soc.* **2009**, *131*, 11686−11688. (f) Ess, D. H.; Goddard, W. A., III; Periana, R. A. Electrophilic, Ambiphilic, and Nucleophilic C−H Bond Activation: Understanding the Electronic Continuum of C−H Bond Activation Through Transition-State and Reaction Pathway Interaction Energy Decompositions. *Organometallics* **2010**, *29*, 6459−6472.

(9) For Woodward−Hoffmann rule, see: (a) Woodward, R. B.; Hoffmann, R. Stereochemistry of Electrocyclic Reactions. *J. Am. Chem. Soc.* **1965**, *87*, 395−397. (b) Hoffmann, R.; Woodward, R. B. Selection Rules for Concerted Cycloaddition Reactions. *J. Am. Chem. Soc.* **1965**, *87*, 2046−2048. (c) Woodward, R. B.; Hoffmann, R. Selection Rules for Sigmatropic Reactions. *J. Am. Chem. Soc.* **1965**, *87*, 2511−2513. (d) Woodward, R. B.; Hoffmann, R. The Conservation of Orbital Symmetry. *Angew. Chem., Int. Ed. Engl.* **1969**, *8*, 781−853.

(10) (a) Sperger, T.; Sanhueza, I. A.; Kalvet, I.; Schoenebeck, F. Computational Studies of Synthetically Relevant Homogeneous Organometallic Catalysis Involving Ni, Pd, Ir, and Rh: An Overview of Commonly Employed DFT Methods and Mechanistic Insights. *Chem. Rev.* **2015**, *115*, 9532−9586. (b) Geerlings, P.; De Proft, F.; Langenaeker, W. Conceptual Density Functional Theory. *Chem. Rev.* **2003**, *103*, 1793−1874. (c) Parr, R. G. Density Functional Theory. *Annu. Rev. Phys. Chem.* **1983**, *34*, 631−656. (d) Davidson, E. R. Computational Transition Metal Chemistry. *Chem. Rev.* **2000**, *100*, 351−352. (e) Demissie, T. B.; Ruud, K.; Hansen, J. H. DFT as a Powerful Predictive Tool in Photoredox Catalysis: Redox Potentials and Mechanistic Analysis. *Organometallics* **2015**, *34*, 4218−4228.

(11) (a) Becke, A. D. Density-Functional Thermochemistry. III. The Role of Exact Exchange. *J. Chem. Phys.* **1993**, *98*, 5648−5652. (b) Lee, C. T.; Yang, W. T.; Parr, R. G. Development of the Colle-Salvetti Correlation-Energy Formula into a Functional of the Electron Density. *Phys. Rev. B: Condens. Matter Mater. Phys.* **1988**, *37*, 785−789. (c) Slater, J. C. *Quantum Theory of Molecules and Solids, Vol. 4: The Self-Consistent Field for Molecules and Solids*; McGraw-Hill: New York, 1974. (d) Vosko, S. H.; Wilk, L.; Nusair, M. Accurate Spin-Dependent Electron Liquid Correlation Energies for Local Spin Density Calculations: a Critical Analysis. *Can. J. Phys.* **1980**, *58*, 1200−1211.

(12) McMullin, C. L.; Jover, J.; Harvey, J. N.; Fey, N. Accurate Modelling of Pd(0) + PhX Oxidative Addition Kinetics. *Dalton Trans.* **2010**, *39*, 10833−10836.

(13) Evans, P. A.; Robinson, J. E. Regio- and Diastereoselective Tandem Rhodium-Catalyzed Allylic Alkylation/Pauson−Khand Annulation Reactions. *J. Am. Chem. Soc.* **2001**, *123*, 4609−4610.

(14) Wang, H.; Sawyer, J. R.; Evans, P. A.; Baik, M. Mechanistic Insight into the Diastereoselective Rhodium-Catalyzed Pauson−Khand Reaction: Role of Coordination Number in Stereocontrol. *Angew. Chem., Int. Ed.* **2008**, *47*, 342−345.

(15) Baik, M.; Mazumder, S.; Ricci, P.; Sawyer, J. R.; Song, Y.; Wang, H.; Evans, P. A. Computationally Designed and Experimentally Confirmed Diastereoselective Rhodium-Catalyzed Pauson−Khand Reaction at Room Temperature. *J. Am. Chem. Soc.* **2011**, *133*, 7621−7623.

DOI: 10.1021/acs.accounts.6b00111
Acc. Chem. Res. 2016, 49, 1263−1270